

# Models of perceptual learning in vernier hyperacuity

Yair Weiss<sup>1</sup>

Shimon Edelman<sup>2,\*</sup>

Manfred Fahle<sup>3</sup>

December 3, 1992

## Abstract

Performance of human subjects in a wide variety of early visual processing tasks improves with practice. HyperBF networks (Poggio and Girosi, 1990) constitute a mathematically well-founded framework for understanding such improvement in performance, or perceptual learning, in the class of tasks known as visual hyperacuity. The present article concentrates on two issues raised by the recent psychophysical and computational findings reported in (Poggio et al., 1992b; Fahle and Edelman, 1992). First, we develop a biologically plausible extension of the HyperBF model that takes into account basic features of the functional architecture of early vision. Second, we explore various learning modes that can coexist within the HyperBF framework and focus on two unsupervised learning rules which may be involved in hyperacuity learning. Finally, we report results of psychophysical experiments that are consistent with the hypothesis that activity-dependent presynaptic amplification may be involved in perceptual learning in hyperacuity.

1. Interdisciplinary Program, Tel Aviv University, Tel Aviv 69978, Israel
2. Department of Applied Mathematics and Computer Science, The Weizmann Institute of Science, Rehovot 76100, Israel
3. Dept. of Neuroophthalmology, University Eye Clinic, Schleichstr. 12, D7400, Tübingen, Germany

★ To whom correspondence should be addressed.

# 1 Introduction

The term “perceptual learning” refers to the significant improvement, precipitated by practice, in the performance of human subjects in various perceptual tasks (Walk, 1978). Some of the more intriguing aspects of perceptual learning, such as its specificity for particular stimulus parameters, and the associated lack of performance transfer to new parameter values (Fiorentini and Berardi, 1981; Karni and Sagi, 1991), remained until not long ago without an adequate computational explanation. In the present report, we show that a recently proposed mathematical framework for learning from examples, known as HyperBF approximation (Poggio and Girosi, 1990), yields a biologically plausible and flexible model of perceptual learning in early vision. Following the work described in (Poggio et al., 1992b), we concentrate on the example of learning vernier hyperacuity.

## 1.1 HyperBF networks

Within the HyperBF framework, the problems of detection and discrimination of visual stimuli are approached in terms of the computation of multivariate functions defined over the input space. In particular, learning to solve these problems is considered equivalent to approximating the value of an appropriate function at any point in the input space, given its values at other points that belong to a set of examples. In a standard implementation, the task of approximating a function is divided into two stages (Poggio and Girosi, 1990): an initial (usually non-linear) transformation, in which the input is mapped into a set of basis functions, and a linear stage, in which the output function is computed as a linear combination of the basis functions.

More precisely, the function  $f(\mathbf{x})$  is approximated as  $\hat{f}(\mathbf{x}) = \mathbf{c} \cdot \mathbf{h}(\mathbf{x})$  where  $\mathbf{h}(\mathbf{x})$  is a vector of the values of the (non-linear) basis functions, and  $\mathbf{c}$  is a vector of weights. It is possible to divide the initial transformation into two sub-stages: a transduction or dimensionality reduction stage, in which the input is mapped into a real vector space  $\mathcal{V}$ , and a basis function computation stage, in which the value of each component of  $\mathbf{h}$  is determined by a function  $h_i : \mathcal{V} \rightarrow \mathcal{R}$ . If the basis functions are radial, then  $h_i(\mathbf{x}) = h_i(\|\mathbf{x} - \mathbf{x}_0\|)$ , where  $\mathbf{x}_0$  are called the centers of the chosen set of basis functions. In a distributed implementation of this scheme by a multilayer network (Poggio and Girosi, 1990),  $\mathbf{h}$  represents the response of units in an intermediate layer to the stimulus, and  $\mathbf{c}$  represents the weights of the synapses between the intermediate layer and the output unit.

## 1.2 Modeling 2AFC experiments with HyperBF networks

Because the output of the HyperBF module is a continuous function of the input, an additional mechanism is needed to model the decision stage in a two-alternative forced choice (2AFC) experiment. For that purpose, the full model (see Figure 1) includes a threshold mechanism that outputs +1 or -1, depending on the sign of its input. Such a threshold unit is likely to be affected by noise, whose source can be, e.g., the spontaneous activity of nearby units (we call this “decision

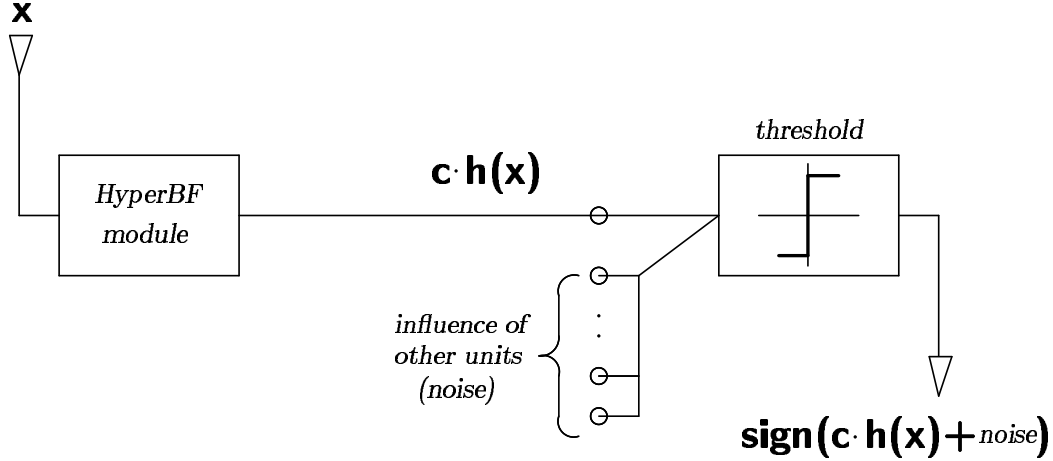


Figure 1: A model of a two-alternative forced choice (2AFC) experiment. The output of the HyperBF module (left) is thresholded. Because the thresholding unit is also affected by the spontaneous activity of other units, only stimuli that elicit a strong response from the HyperBF network will be detected correctly with a high probability.

noise,” as opposed to “early noise” which is already present in the values of the basis functions  $\mathbf{h}(\mathbf{x})$ ). Thus, the output of the threshold unit can be described by  $R(\mathbf{x}) = \text{sign}(\mathbf{c} \cdot \mathbf{h} + DN)$ , where  $DN$  is a zero-mean normal random variable with a standard deviation  $\sigma_N$ .

Given the distribution of the noise in the system, it is possible to calculate the performance of the model in a 2AFC experiment. For example, if  $Y$  is the response of the HyperBF module to a certain right-offset vernier, and if early noise is neglected, the probability of a correct response is:

$$\begin{aligned}
 Prob_{\text{correct}} &= Prob(DN + Y > 0) \\
 &= \int_{-\infty}^Y e^{-1/2(\frac{s}{\sigma_N})^2} ds \\
 &\doteq \Phi(Y/\sigma_N)
 \end{aligned} \tag{1}$$

The offset threshold of the model is then defined as the smallest offset,  $o_T$ , for which the probability of correct responses as defined above is above 0.75. If the network’s output depends on the input offset in an almost linear fashion (see Figure 4), then the psychometric curve and the threshold can be predicted analytically. Substituting  $Y(o) = ao$  in equation 2 gives:

$$\begin{aligned}
 Prob_{\text{correct}}(o) &= \Phi(ao/\sigma_N) \\
 Prob_{\text{correct}}(o_T) &= 0.75 \Rightarrow \\
 o_T &= \frac{1}{a}\sigma_N\Phi^{-1}(0.75)
 \end{aligned} \tag{2}$$

The percentage of correct responses plotted against the input offset will then be a sigmoid, and the threshold will be inversely proportional to  $a$ .

Although the above approach makes it possible to model both interpolation and decision performance, we chose to concentrate on the former. This choice was motivated by the assumption that the interesting aspects of learning have to do with changes in the performance of the interpolation module. In the modeling of vernier acuity, this assumption is supported by the psychophysical findings of stimulus specificity of learning, which cannot be accounted for by decision-level changes alone (Poggio et al., 1992b).

### 1.3 Vernier hyperacuity

A vernier target consists of two line segments, separated by a small offset in the direction orthogonal to the orientation of the lines. The subject’s task in a vernier acuity experiment is to judge whether the misalignment is to the left or to the right. Humans solve this task successfully when the offset is as small as 5" or less, exhibiting a discrimination threshold that is far lower than that for spatial frequency grating discrimination or for two point resolution, and smaller than the spacing of the cones in the fovea. Moreover, this astonishing precision of vernier discrimination, termed hyperacuity, is maintained even when the target is in motion (Westheimer and McKee, 1975). It should be noted that hyperacuity performance does not contradict any physical law, since the optics of the eye at the fovea satisfy the constraints of the sampling theorem, making the spatial information recoverable in principle, by appropriate filtering (Barlow, 1979; Crick et al., 1981).

Our choice of vernier hyperacuity as a paradigmatic case of perceptual learning was motivated by two considerations. First, the improvement in the vernier threshold has both fast and slow components (McKee and Westheimer, 1978; Fendick and Westheimer, 1983; Fahle and Edelman, 1992), signifying that a number of distinct learning mechanisms may be at work. Second, as we have already mentioned, perceptual learning in vernier hyperacuity is specific for stimulus orientation (Fahle and Edelman, 1992), a possible indication that performance in this task is based, at least in part, on interpolation among input examples acquired during learning. The next two sections describe in detail a computational model of hyperacuity performance based on HyperBF interpolation.

## 2 Modeling hyperacuity-level performance

### 2.1 Simulated experiments

In the simulated psychophysical experiments described below we compared two versions of the HyperBF scheme, one without and the other with a preprocessing or transduction stage. Unlike in (Poggio et al., 1992a) where a transduction stage was used, in version A of the present model the

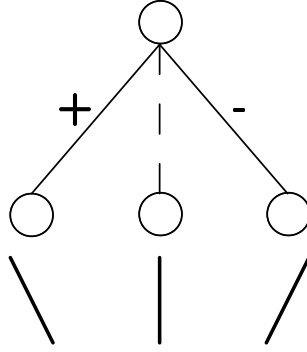


Figure 2: A simple network for vernier discrimination, obtained by combining responses of orientationally selective units. If the parameters of the oriented units are set according to the data from psychophysical masking experiments (Wilson and Gelb, 1984), this network can solve the vernier task at a much smaller threshold than the size of the excitatory region of each unit. This network is only suitable for solving the vernier task when the stimulus is vertically oriented. Networks that combine responses of a range of orientationally selective units can be used for stimuli of different orientations.

basis function vector  $\mathbf{h}$  represented the activities of three orientation-selective units, with response peaks at  $-15^\circ$ ,  $0^\circ$  and  $15^\circ$  with respect to the vertical. The response of each unit was calculated by convolving the stimulus retinal image with the appropriate receptive field function  $RF(x, y)$  and adding noise  $EN$ :

$$h_i = \int \int RF_i(x, y)I(x, y)dx dy + EN$$

For the  $0^\circ$  unit  $RF(x, y) = e^{-y^2/\sigma_y^2}(e^{-x^2/\sigma_1^2} - Be^{-x^2/\sigma_2^2} + Ce^{-x^2/\sigma_3^2})$ . Equations for the  $\pm 15^\circ$  units were obtained using standard rotation of coordinates. All constants were taken from (Wilson and Gelb, 1984) as those representing the smallest spatial frequency channel in human subjects. These constants are based on masking experiments, and are consistent with data from single cell recordings in macaque striate cortex (Wilson, 1986; Wilson and Gelb, 1984).  $EN$  was a zero mean Gaussian random variable. The responses of these three basis functions to a sequence of vernier stimuli (a “vernier tuning curve”) is shown in figure 3, along with a more conventional orientation tuning curve for the vertically oriented unit.

In version B, the orientation-selective units described above were considered as transducers that mapped the activity pattern of the retinal array into  $\mathcal{R}^3$ . The network solved the problem by carrying out Radial Basis Function interpolation in  $\mathcal{R}^3$ . The basis functions comprising  $\mathbf{h}$  were three Gaussians in  $\mathcal{R}^3$ , centered around the transduced representations of three vernier stimuli with offsets of  $-30, 0, 30$  arcsec, respectively. The widths of the Gaussians were set to the average distances (in  $\mathcal{R}^3$ ) between their centers.

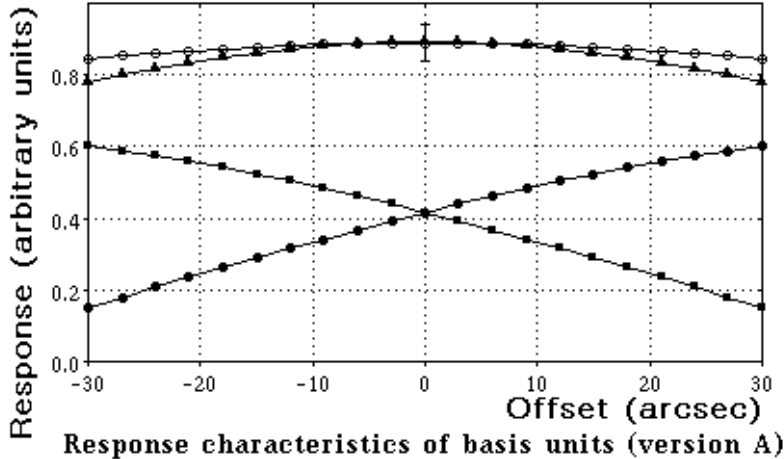


Figure 3: “Single-cell recordings” from the basis units in the network, for a range of vernier offset values. The three curves marked by filled symbols are the responses to vernier stimuli of the three orientation-selective units shown in Figure 2. The error bar shows the standard deviation of the noise used to obtain the response curve shown in figure 4. For comparison, the response curve of the vertically oriented unit to an unbroken line passing through the midpoints of the two lines comprising the vernier target is also shown (the top curve, marked by circles). The network treats such oriented line as equivalent to a vernier target. Single-cell recordings from area 17 of a cat’s visual cortex (Swindale and Cynader, 1986) have revealed similar response patterns.

In both versions the weight vector  $\mathbf{c}$  was obtained by solving the equation:

$$\mathbf{H}\mathbf{c} = \mathbf{Y} \tag{3}$$

where each row in the matrix  $\mathbf{H}$  represents the activity of the hidden layer to a vernier stimulus, and  $Y_i$  is set to  $-1$  for left offsets and to  $+1$  for right offsets.

## 2.2 Results

We first explored the response of the network to vernier stimuli consisting of two lines  $8'$  long. In both versions, the weight vector  $\mathbf{c}$  was of the form  $\alpha(1, 0, -1)^T$  and the network could be described simply as an output unit with an excitatory synapse with the unit tuned to the left-slanting lines and an inhibitory synapse with the unit tuned to the right-slanting lines (see figure 2). The zero weight of the vertically oriented unit is due to the fact, pointed out by Wilson, that this unit,

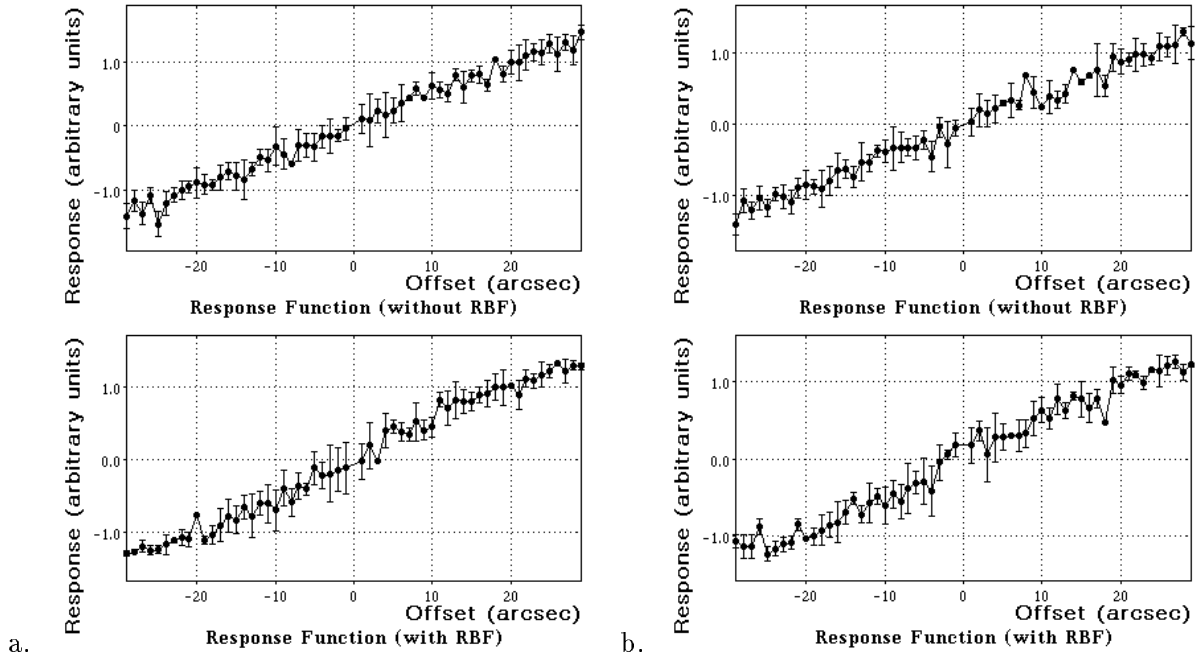


Figure 4: *a*, Response of the network plotted vs. the vernier offset of a stimulus presented at a fixed location with respect to the receptive fields. The two versions, A and B (top and bottom rows), yielded similar results here. *b*, Response of the network vs. the vernier offset of a stimulus presented at random locations within a  $20''$  horizontal range around the common center of the receptive fields.

despite being the most active one, carries the least amount of information relevant to the solution of the task.

The output of this network for offsets ranging from  $-30''$  to  $30''$  is shown in Figure 4a. These graphs represent the response of the network to a vernier stimulus centered over the orientation detectors. In practice, however, random eye movements of the subject prevent such precise centering of stimuli during psychophysical experiments. Figure 4b shows the network's responses to stimuli displaced by random displacements of up to  $20''$  in the vertical and horizontal directions.<sup>1</sup> It can be seen that the network's output is little affected by stimulus location. Interestingly, while the network is sensitive enough to signal a vernier displacement of only  $1''$ , it practically ignores a much larger translation of the entire stimulus.

Note that in both cases the network's output depends on the input offset in an almost linear

<sup>1</sup>The distance between units that were spatial nearest neighbors was used by Wilson and Gelb (Wilson and Gelb, 1984) as a free parameter to fit spatial frequency discrimination data. For the filters we used in our model, this distance corresponded to  $38.3''$ . Thus, a stimulus appearing at a random retinal location would always be within  $20''$  of a set of filters.

fashion, while the function to be approximated,  $f(\mathbf{x})$ , is a step function. Such poor approximation of the target function is understandable, considering the smoothness of the basis functions. A much better approximation could be reached using discontinuous basis functions, or, alternatively, using a large number of narrow Gaussian basis functions.

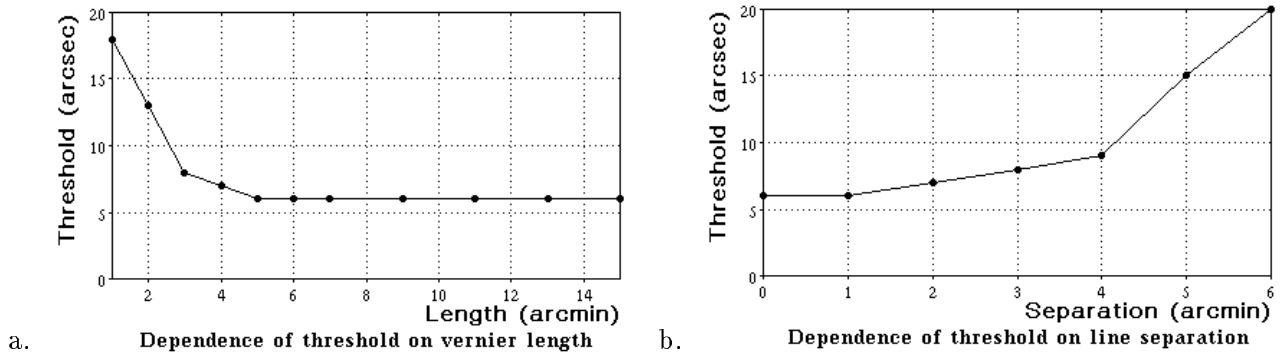


Figure 5: Dependence of vernier threshold on line length (*a*) and separation between lines (*b*). Threshold was estimated by making assumptions regarding the statistical distributions of the noise sources. These distributions were held fixed as stimulus parameters varied. Compare to Figure 6.

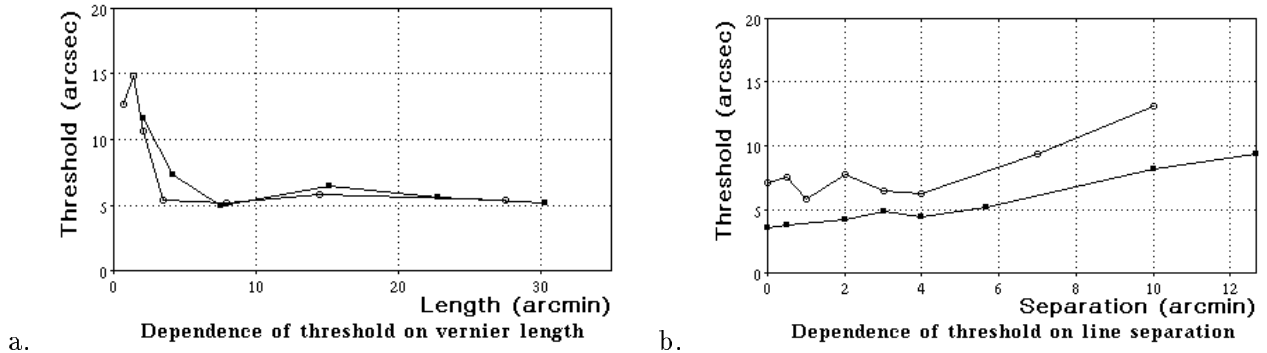


Figure 6: Dependence of vernier threshold on line length (*a*) and separation between lines (*b*). Each plot show data from two observers, replotted from (Westheimer and McKee, 1977).

### 2.3 Discussion

Since both versions of the model (A and B) can serve as the basis for hyperacuity level performance, we adopted the simpler, linear, version that omits the transduction stage, as a minimalist platform for studying the improvement of hyperacuity with practice.

The primary motivation for using oriented filters as basis functions for vernier hyperacuity, was the report by Wilson ((Wilson, 1986) see also (Klein and Levi, 1985; Watt and Morgan, 1985)) that the responses of these filters can explain psychophysical data concerning hyperacuity.



In Wilson’s model, detection threshold in psychophysical experiments is related to the Euclidean distance between a distributed “filter representation” of the two stimuli. The filter representation is constructed by pooling the responses of filters at all orientations and spatial frequencies concentric with the stimulus as well as over spatial nearest neighbors. Our model, in contrast, replaces the distributed representation with the output of a single neuron. This does not necessarily make our model more biological, but it makes it easier to model hyperacuity learning in terms of synaptic modification.

Wilson’s model replicated several psychophysical results concerning the change in hyperacuity thresholds in a variety of hyperacuity tasks when stimulus parameters varied. To see whether these results still hold when the distributed representation is collapsed to a single neuron, we investigated the response of the network to verniers of varying line length and varying gap in the direction of the lines. The results of these simulations appear in Figure 5. In these simulations the statistical distribution of the noise was held fixed (and thus thresholds could be estimated) while the parameters of the stimulus varied. The dependence of the threshold on line length exhibited by the model agrees reasonably well with the data in (Westheimer and McKee, 1977). Specifically, the threshold decreases steeply with increasing segment length for lengths under  $4'$ , and is essentially unaffected by further increase. The dependence of the threshold on line separation, however, agrees with psychophysical data only qualitatively. The model’s threshold increases steeply for separations greater than  $4'$ , while in human subjects the increase is more gradual and is especially noticeable for separations over  $7'$ . Both the results regarding line length and line separation can be attributed to the fact that the width  $\sigma_y$  of the spatial frequency mechanism used by the model was  $3.65'$  (Wilson and Bergen, 1979). As Wilson has pointed out, increasing line length beyond the value of  $\sigma_y$  does not add any significant information, while increasing line separation beyond  $\sigma_y$  forces the human subject to use the less sensitive spatial mechanisms.

Additional motivation for using orientationally selective units as basis functions in our model comes from the electrophysiological studies of Swindale and Cynader (1986), who studied the response to a vernier break by orientation selective cells in cortical area 17 in the cat. The results of that study showed that orientation-selective cells in area 17 can discriminate between different offsets in a vernier stimulus. Specifically, those cells tended to respond to the vernier stimuli in the same manner as they did to an oriented line passing through the midpoints of the two segments composing the vernier. This effect is basically due to the spatially low-pass action of the orientationally selective units, and has been replicated by our model (Figure 3).

Swindale and Cynader used a method proposed by Parker and Hawken (1985) to estimate the “hyperacuity threshold” of single neurons in area 17. This threshold measures the statistical reliability of a change in a neuron’s response to a vernier break. Because the thresholds of some neurons were as low as the behavioral threshold of the cat in vernier discrimination, the authors suggested that the performance of these neurons was the limiting factor in hyperacuity, obviating

the need for a fine-grid reconstruction of the stimulus. In response, Parker and Hawken (1987) argued that the possibility of a fine-grid reconstruction could not be ruled out, because the factors limiting the behavioral hyperacuity threshold may be retinal and not cortical, as suggested by the data on the hyperacuity thresholds of cat retinal ganglion cells due to Shapley and Victor (1986).

We note that the HyperBF approach is equally capable of modeling retinally or cortically based hyperacuity mechanisms. While our present model used orientationally selective units similar to cortical simple cells, the HyperBF scheme of (Poggio et al., 1992a) that relied on responses of circularly symmetric units was equally successful in replicating hyperacuity phenomena. The notion of interpolation, inherent to the HyperBF approach, does provide, however, a useful insight into one issue important for both sides in the retina vs. cortex debate, namely, the way of relating behavioral thresholds to those of single neurons.

Consider the vernier tuning curve of the vertically oriented unit in our model (the curve marked by triangles in figure 3). Despite the fact that this curve is relatively wide and shallow, the responses of three units of this type can support hyperacuity vernier discrimination. Addressing Westheimer’s (1981) claim that neurons with a wide orientation response characteristic cannot be involved in hyperacuity tasks, Swindale and Cynader argue that a broadly tuned neuron can still support hyperacuity, as long as its response pattern is statistically reliable. This is equivalent to saying that the slope of the tuning curve, and not its width, should be used as a measure of a neuron’s use for hyperacuity.

In contrast, our model suggests that neither measure should be considered a sole determinant of the behavioral threshold: the responses of cells slightly rotated with respect to the stimulus actually provide more relevant information for solving the task. Thus, a network of very reliable vernier detectors may perform worse than a network of less reliable units with a large overlap in their receptive fields. The limiting factor in the vernier task seems therefore to be not the performance of a single unit, but rather the ability of the system to pool responses from different units with overlapping receptive fields, and the manner in which these units cover the range of possible stimulus orientations (see figure 7).<sup>2</sup> To conclude this discussion, we note that Snippe and Koenderink (1992) have recently demonstrated analytically, using an ideal observer model, that the resolution of a channel-coded system of circularly symmetric receptive fields is determined both by the reliability of each channel and by the degree of overlap between the channels.

---

<sup>2</sup>Swindale and Cynader mention pooling the outputs of several neurons, but they suggest that this pooling occurs between neurons with similar responses, thus increasing the reliability of a single channel, and not pooling the responses of different channels.

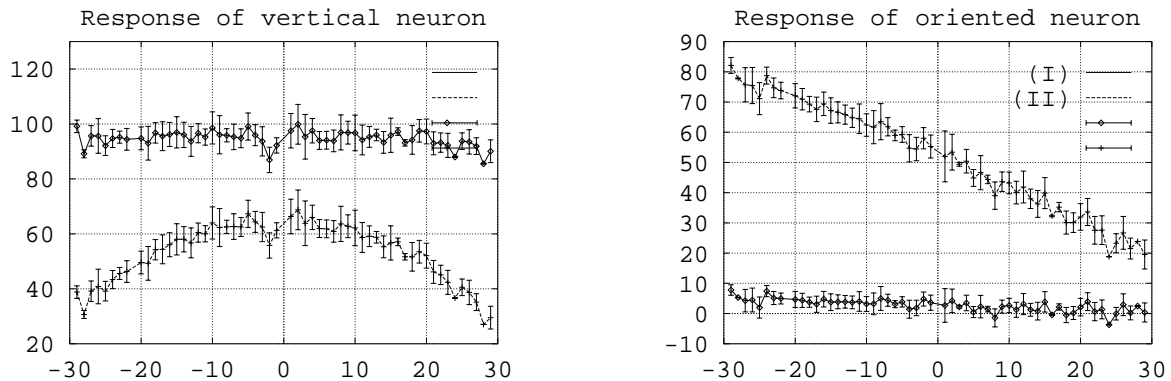


Figure 7: To demonstrate the importance of pooling responses of a number of overlapping filters, we conducted two simulations in which the output of the filters was passed through a monotonic nonlinearity before noise was added. In the first simulation, the nonlinearity was compressing at high activity rates, resulting in a shallow vernier tuning curve. In the second simulation, the nonlinearity was accelerating at high activity rates, leading to a steep vernier tuning curve. *a* The average response of two simulated neurons to vernier displacements in a vertically oriented stimulus (lower curve: type I; upper curve: type II). *b*. The average response of two simulated neurons with the same nonlinearity as those in *a* but with oriented receptive fields. A network comprised of three neurons of type II (upper curve) performs better in the vernier task than a network comprised of three neurons of type I (lower curve), despite having a shallower vernier tuning curve.

### 3 Modeling perceptual learning in hyperacuity

We now turn to explore the possible ways in which the performance in the vernier task could be made to improve with practice. First, we show how different types of learning rules can be formulated within the HyperBF framework. We then focus on two likely candidate mechanisms for unsupervised learning in vernier acuity experiments, and describe additional simulations which help distinguish between them. The results of these simulations suggested a psychophysical experiment, reported in the next section. We also discuss a possible biological basis for one of the two unsupervised learning rules.

#### 3.1 Classification of perceptual learning models

Perceptual learning models can be categorized according to two basic criteria: how much prior knowledge is assumed and how dependent the learning is on external supervision. Both parameters can assume a wide range of values, a fact which is sometimes overlooked when models are characterized simply as “supervised” or “unsupervised.”

Supervised models, in turn, may differ in the nature of feedback signal they assume. Barto (1989) distinguishes between two types of error signals — those generated by a “teacher” that can point out which parameter of the model should be modified in response to the error it has committed, and those generated by a “critic” that is unaware of the workings of the model. “A critic can generate a payoff based on knowledge solely of *what* it wants accomplished and not of *how* the learning system can accomplish it” ((Barto, 1989), p.89). Unsupervised models can also differ in their dependence on feedback. Some unsupervised models merely replace the external feedback signal with a self-provided feedback signal, an “internal teacher.” Alternatively, an unsupervised model can assume complete independence on feedback, either internal or external.

A fundamental tradeoff exists between a learning model’s reliance on prior knowledge and on feedback. A model that relies heavily on a teacher can afford to make few prior assumptions, while a model that assumes independence from feedback must rely on prior knowledge to a greater extent. As an example of feedback-independent unsupervised learning, consider the model of hyperacuity, proposed by Barlow and others (Barlow, 1979; Crick et al., 1981), that relies on a fine-grid reconstruction of the retinal signal in the cortex. Assume that the module that processes the reconstructed signal has no intrinsic capacity for learning, but operates in such a manner that increasing the accuracy of the fine-grid reconstruction causes an improvement in its performance in the hyperacuity task. Any improvement in the fine-grid reconstruction would then cause a decrease in hyperacuity threshold, but this improvement need not be feedback-dependent. Indeed, the reconstruction may improve after training on a completely different task.

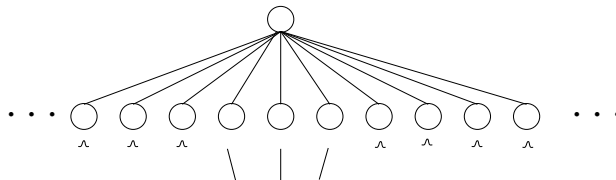


Figure 8: The structure of the network used throughout the learning simulations. The output neuron receives input from 100 neurons, three of which correspond to the properly oriented and positioned linear filters, and the rest to other, random, inputs. Performance is improved by modifying the connections between these neurons and the output neuron.

### 3.2 Different learning modes in a HyperBF network

In (Poggio et al., 1992a), a HyperBF network was synthesized from a “tabula rasa” initial state. Only the shape of the basis functions (that were radially symmetric multidimensional Gaussians) was assumed to be given. The centers of the basis functions were determined by the training examples in an unsupervised fashion, while the coefficients  $\mathbf{c}$  were updated using a pseudoinverse

technique that assumed an external teacher. Poggio et al. also suggested using self-provided feedback to replace the external teacher.

In our model, the structure of the network was assumed to remain fixed throughout training. The network (see figure 8) was comprised of 100 units which were connected to an output neuron. Three of the units represented the oriented linear filters described in section 2.1 and the activity of the remaining units was random. The model’s performance was improved solely by changing the weight vector  $\mathbf{c}$ , according to four different update rules:

1. The Widrow-Hoff rule.  $\mathbf{c}^{(t+1)} = \mathbf{c}^{(t)} + \eta \mathbf{h}(Y(\mathbf{x}) - O(\mathbf{x}))$ , where  $Y$  and  $O$  represent the desired and the actual output for the stimulus  $\mathbf{x}$ . This rule is supervised by a teacher, and is equivalent to solving equation 3 by an incremental pseudoinverse technique (Widrow and Stearns, 1985).
2. The Mel-Koch rule.  $\mathbf{c}^{(t+1)} = \mathbf{c}^{(t)} + \alpha \mathbf{h}Y(\mathbf{x}) - \beta \mathbf{c}^{(t)}$ . This learning rule was suggested by Mel & Koch (1990) and was designed to maximize the correlation between the output and the activities of the basis function units, while minimizing the total synaptic weight of the linear stage. This model, unlike the previous one, is supervised by a critic who knows only what the correct answer should be.
3. The self-supervised Widrow-Hoff algorithm. This algorithm is similar to the first one, but feedback is provided only for those inputs in which the vernier offset exceeds the baseline threshold (set at  $15''$ ). This model is unsupervised, but is still feedback-dependent. It was designed to simulate the conditions in psychophysical experiments in which subjects receive no feedback at all, but nevertheless possess a clear indication of the correctness of their response for the large values of vernier offset when the stimulus looks trivially easy. Under these conditions, the subjects’ thresholds improve with practice, albeit at a slower rate than when explicit feedback is available (Fahle and Edelman, 1992).
4. Exposure-Dependent Learning (EDL).  $c_i^{(t+1)} = c_i^{(t)} + \alpha c_i^{(t)}$ , if  $|h_i^{(t)}| > \epsilon$ . This is an unsupervised, use-dependent rule, which is independent of feedback. As opposed to the rules listed above, which made no assumptions about the nature of the connections  $\mathbf{c}$  prior to learning, this rule assumes that the weight vector for the oriented filters is proportional to  $(+1, 0, -1)^T$ .

### 3.3 Results

The learning curves for the four rules described in the previous section are shown in figure 9. All rules except one showed a gradual improvement of performance with practice.<sup>3</sup> The shapes of

---

<sup>3</sup>The failure of Mel & Koch’s rule to converge was not due to simulation details. An analysis of their rule formulated as a first-order differential equation showed that it was not guaranteed to converge under the conditions of the simulated experiments, in which widely differing inputs are presented in alternation.

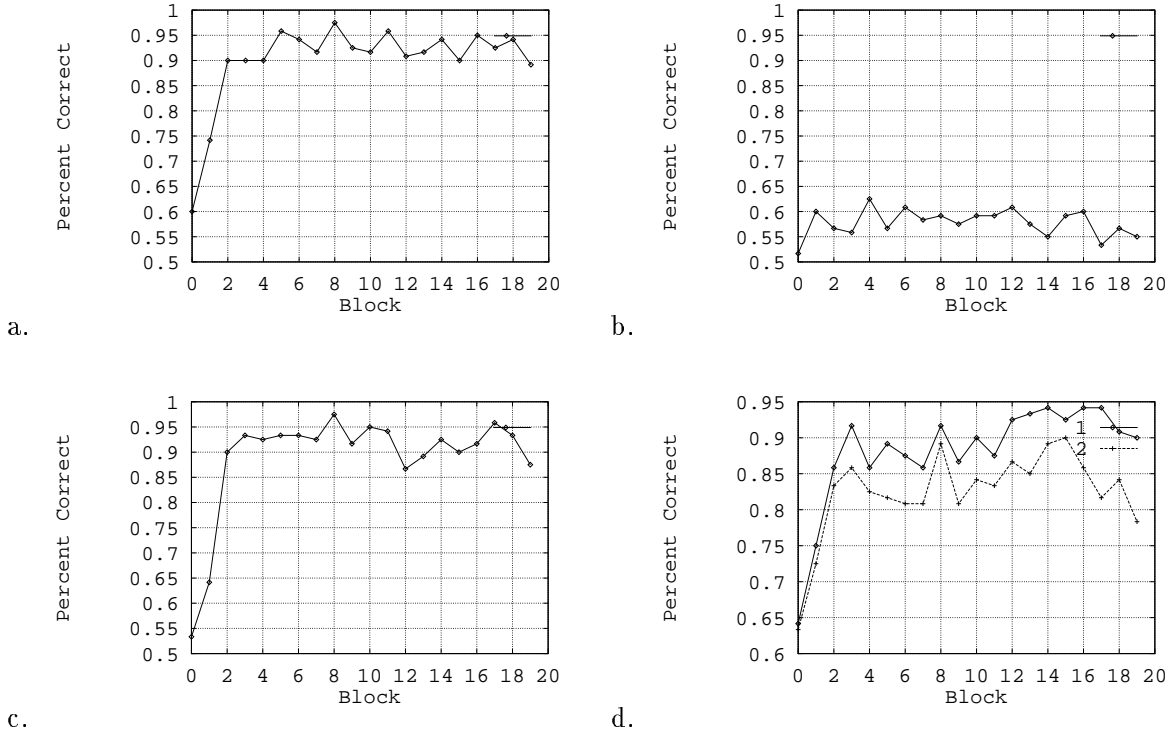


Figure 9: Learning curves for different coefficient-learning rules defined in section 3.2 (*a*: Widrow-Hoff; *b*: Mel-Koch; *c*: self-supervised Widrow-Hoff; *d*: EDL). All rules (except the Mel-Koch rule) show a gradual improvement of performance with practice. The models do not achieve perfect performance due to the noise present in the receptor activities (“early noise”). When this noise is increased, performance still improves, but the final performance level is lower (see the lower curve in condition d).

the learning curves should be considered as a qualitative characteristic of the models’ performance, since they depend on the scalar parameters  $\eta$  and  $\alpha$  (we note that a considerable variability in the learning rate is also found in human subjects). The models do not achieve perfect performance due to the noise present in the receptor activities (“early noise”). When this noise is increased, performance still improves, but the final performance level is lower (see the lower curve in figure 9d).

### 3.4 Separating the noise from the signal: two approaches

Of the four learning rules mentioned in the previous section, the two likely candidates for accounting for the improvement with practice found in psychophysical experiments are the two unsupervised rules, because learning has been found to occur in the absence of feedback. To help elucidate the difference between the two learning rules, we conducted an additional set of learning simulations.

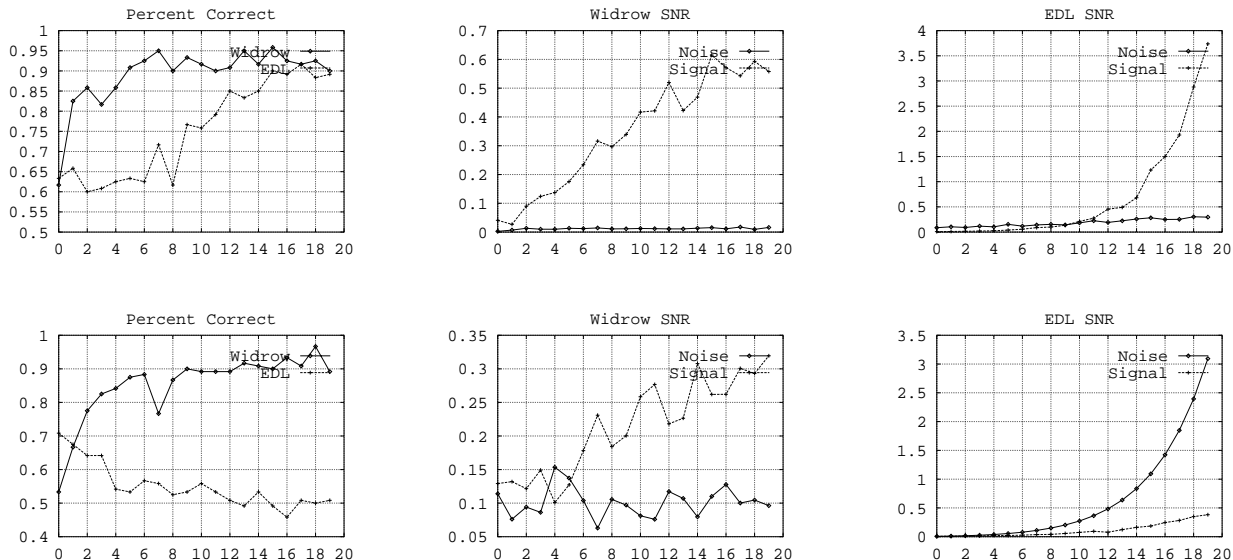


Figure 10: A comparison of the two unsupervised learning rules under two conditions. One where the activity of noisy neurons was determined randomly before each presentation, and the other where they remained constant during learning. The Widrow-Hoff algorithm causes improved performance under both conditions but the EDL algorithm does not improve in the second condition, since it tends to amplify the noise rather than the signal.

These simulations compared the performance of the two learning rules under two conditions which differed only in the firing patterns of the “noise” units. In both conditions, these firing patterns were determined using a zero mean Gaussian random variable. In the first condition (condition A) these firing rates were determined before each presentation of the stimulus (this condition is identical to the one used in the simulations in the previous section) while in the second condition (condition B) these firing rates were determined prior to training and remained constant throughout training. Note that if each presentation is considered by itself, the statistical properties of the “noise neurons” are identical (independent, identically distributed Gaussians).

### 3.4.1 Results

The behavior of the two learning rules under these two conditions is illustrated in figure 10. The first column shows the percentage of correct responses for the two learning rules. The Widrow-Hoff rule supports learning under both conditions, but the EDL rule does so only in condition A, and actually leads to deterioration of performance with practice in condition B.

The second and the third columns show the evolution of signal and noise magnitudes during training. These were defined as:

$$S = E \left[ \sum_{i=1}^3 c_i(t) h_i(t) \right]^2$$

$$N = E \left[ \sum_{i=4}^{100} c_i(t) h_i(t) \right]^2$$

where indices  $i = 1, 2, 3$  correspond to the oriented filters. Note that the term “signal” for the value  $S$  is somewhat misleading since it also includes the contribution of early noise present in the receptors.

The difference between the two learning rules is in the way they distinguish signal from noise. The Widrow-Hoff algorithm converges to a vector  $\mathbf{c}$  such that  $\mathbf{c} \cdot \mathbf{h}$  is closest in the mean square sense to the desired output. Thus, presynaptic activity which is completely uncorrelated with the desired output will result in a zero-weight synapse, in effect labeling the corresponding presynaptic unit as noise. Note that according to this definition, the activity of the vertically oriented filter is also labeled as noise, and indeed the Widrow-Hoff algorithm results in a zero-weight synapse between the vertically oriented filter and the output unit.

A feedback-independent learning rule such as EDL cannot rely on the correlation between the desired output and the presynaptic activity in distinguishing noise from signal. The heuristic used by this rule is to label as signal those inputs which are consistently active at a significant rate when the stimulus is presented. This is achieved by increasing by a small amount the contribution of a unit whose activity is greater than some threshold  $\epsilon$  at each presentation. Thus, when the activities of the random units are recalculated prior to each stimulus presentation, the increase in their contribution to the output unit is negligible compared to the increase in the contribution of the oriented filters (see figure 10), because only the oriented filters are consistently active. In contrast, in condition B, the number of noise units whose activity is greater than  $\epsilon$  is the same as in condition A, but the increase in the contribution of the noise units is significant, due to the consistent activity of the same noise units. In the simulations described above, the number of random units with activity greater than  $\epsilon$  was greater than the number of oriented filters, so that in condition B noise was boosted more than the signal, resulting in decreased performance.

### 3.4.2 A possible biological basis of the EDL rule

The EDL update rule requires a modulatory signal to mark the time frame within which presynaptic activity should be measured, and a mechanism for updating synapses based on presynaptic activity. A learning rule that satisfies these requirements has been studied extensively both at the behavioral and at the cellular level by Hawkins, Abrams, Carew, and Kandel (1983) in *Aplysia*.



The Aplysia’s gill withdrawal reflex following stimulation of a particular site on the siphon was found to be enhanced by a shock delivered to the tail in parallel with the stimulation of the siphon. This enhancement was specific to the site which was stimulated at the time of the shock delivery to the tail, presumably because it depended on simultaneity of the shock and the siphon stimulation.

A correlate of this phenomenon at the cellular level was found in a study of the change of the excitatory postsynaptic potentials (EPSPs) elicited in a common postsynaptic neuron by siphon sensory neurons. During training, two sensory neurons were stimulated intracellularly. Stimulation of one of them immediately preceded the shock to the tail, while stimulation of the other sensory neuron followed the shock by 2.5 minutes. It was found that the change in the amplitude of the EPSP from the paired neuron was significantly greater than that in the unpaired neuron. Further experiments suggested that “activity-dependent amplification of facilitation is presynaptic in origin and involves a differential increase in spike duration and  $\text{Ca}^{2+}$  influx in paired versus unpaired neurons” (Hawkins et al., 1983).

The requirements of the model of Hawkins et al. are: (i) facilitatory neurons, which are excited by motivationally significant stimuli and which may project very diffusely (in principle, a single such neuron that produced facilitation in all of the sensory neurons would be sufficient to explain the results) and (ii) differential activity in the neurons that receive facilitatory input (Hawkins et al., 1983). In our simulations we assumed that all the units received the modulatory signal, that is, the network had no *a priori* knowledge as to the activities of which units were more likely to be significant.

The main difference between our mechanism and the one suggested by Hawkins et al. is that we assume that when synaptic amplification occurs, it is proportional to the previous synaptic strength. Without this assumption, the modification of the synapses distorts whatever structure the network connections had prior to learning. For example, the connections of the vertically oriented unit, which is irrelevant to the task, would also increase if this assumption were dropped. We note that this assumption adds a Hebbian element to the learning rule. Consider two units with identical activity, one of which has a strong connection to the output unit and consistently takes part in the activation of the output unit, and the other is weakly connected to the output. The synaptic weight of the strongly connected unit, whose activity is correlated with the output, would increase more significantly than that of the weakly connected unit. We do not assume, however, that there is any *causal* relationship between the correlation of pre- and postsynaptic activities, and the synaptic modification. Hence, our rule may be classified as a “non-interactive Hebbian rule” (Brown et al., 1990).

## 4 Psychophysical experiments

In the previous section, we described the difference between the two unsupervised learning rules in terms of their approach to distinguishing between signal and noise. If a group of units is consistently active during stimulus presentation, but their activities are uncorrelated with the desired output, then they would be labeled as noise by the Widrow-Hoff algorithm and as signal by the EDL rule.

To elucidate the possible role of an EDL-like rule in the improvement of performance in vernier hyperacuity, we conducted psychophysical experiments using cross-shaped stimuli shown in figure 11. Two orthogonal verniers appeared simultaneously in each trial, but the subjects were required to judge the sense of the misalignment of only one of the two verniers (the orientation of the relevant vernier was the same throughout each experimental block). In this situation, the units responsive to the irrelevant part of the stimulus are consistently activated during stimulus presentation, but their activity is uncorrelated with the desired output. Hence, if the learning mechanism contains a significant use-dependent component (of the kind that can be provided by the EDL rule), such an experiment is expected to demonstrate similar improvement with practice in the two orientations.

### 4.1 Method

Subjects performed three tasks that involved cross-shaped stimuli as in figure 11. Stimuli were generated and displayed on a Silicon Graphics 4D35/TG workstation. Viewing distance was such that one pixel corresponded to about  $8''$ . Stimuli were presented for  $100ms$  and were separated by a  $1sec$  interval (during which a frame was displayed to assist fixation). Subjects indicated their response by pressing one of two buttons on the computer mouse. Auditory feedback was given for incorrect responses.

The stimuli in the first two tasks, HORIZONTAL CROSS and VERTICAL CROSS, were the same, except that in one (VERTICAL CROSS) subjects were required to determine the direction of misalignment of the vertical part of the stimulus (and received appropriate feedback), while in the other (HORIZONTAL CROSS) they were required to judge the misalignment of the horizontal part of the stimulus (again with appropriate feedback). In the third task, DIAGONAL CROSS, the stimuli were oriented diagonally.

Each block consisted of a fixed number of presentations of all offsets of the relevant stimulus (in the range from  $-20$  to  $+20$  pixels) in a random order of presentation. The irrelevant part of the stimulus (e.g., the vertical vernier in a HORIZONTAL CROSS block) was presented with a random offset and was thus uncorrelated with the error signal. The experiments consisted of three stages:

- Measurement of baseline performance in all three tasks.
- Training in either the vertical or horizontal tasks.

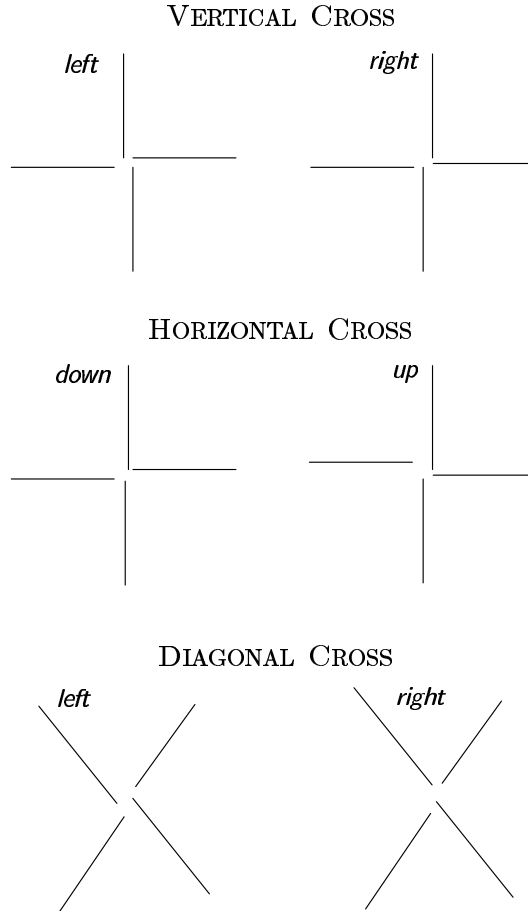


Figure 11: The stimuli used in the experiments were similar to those seen above. In each block observers were shown vertical, horizontal or diagonal crosses with randomly varied offsets.

- Testing in the two tasks for which there was no training.

The diagonal task was added only after the first two subjects had completed the experiment, and they were called back for an additional block of testing. Before they were tested on the diagonal cross, we assessed their performance on the horizontal cross to determine whether they retained their learning despite the elapsed time (10 days for observer YK and 45 days for observer FL).

## 4.2 Results

Results are shown in table 1. Because of the extensive coverage of the range of offsets (all offsets smaller than 20 pixels were presented in each block), we were able to plot the observers' psychometric curves in each block. For some observers (see figure 12), these curves assumed the usual sigmoid shape only after training. For this reason, we measured the observers' performance by the percentage of correct responses in a range of offsets kept constant throughout training, rather than

by a threshold estimated via probit analysis.

As in previous experiments on perceptual learning, individual differences in the learning rates could be observed. When learning did occur for the attended part of the stimulus, it was accompanied by a significant improvement for the part that was present throughout training but was uncorrelated with the feedback. No such concomitant improvement was found after training in the diagonal test stimulus, which was not present in training (but note that only the results of observer RM in the diagonal tasks serve as a true control, as the others were either not tested for baseline or did not learn at all).

Observer FL apparently did not retain his performance after a prolonged time break, while observer YK showed a much smaller decrease in performance. Observer YA explained that when tested on the vertical task (following training on the horizontal task) she tried to find a hidden cue in the horizontal verniers displayed simultaneously with the vertical verniers. Since these verniers were uncorrelated with the correct response, this explains the deterioration of her performance on the vertical task.

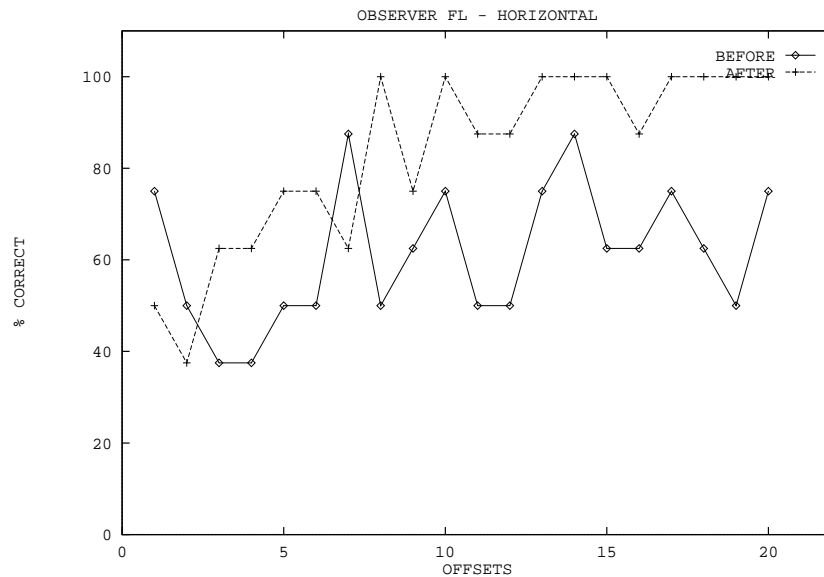


Figure 12: Representative psychometric curves (observer FL) before and after learning in the horizontal task. The response curves start to resemble a sigmoid only after training.

### 4.3 Discussion

These results are consistent with a use-dependent learning rule such as EDL. Note that this rule still predicts that learning will be stimulus-specific and will not transfer to new tasks, but it distinguishes

Subject	Training	<i>Horizontal</i>		<i>Vertical</i>		<i>Diagonal</i>	
		<i>before</i>	<i>after</i>	<i>before</i>	<i>after</i>	<i>before</i>	<i>after</i>
FL	vertical	61 $\pm$ 1.8	83 $\pm$ 0.64 (67)	59 $\pm$ 1.2	75 $\pm$ 0.85	-	58 $\pm$ 1.5
YK	vertical	78 $\pm$ 1.33	91 $\pm$ 0.5 (88)	67 $\pm$ 1.7	77 $\pm$ 1.1	-	75 $\pm$ 1.2
YA	horizontal	85 $\pm$ 1.0	87 $\pm$ 0.7	76 $\pm$ 1.4	71 $\pm$ 1.3	75 $\pm$ 1.5	76 $\pm$ 1.1
RM	horizontal	70 $\pm$ 1.6	78 $\pm$ 1.1	75 $\pm$ 1.4	84 $\pm$ 0.8	86 $\pm$ 0.9	83 $\pm$ 0.9
AS	horizontal	81 $\pm$ 1.2	83 $\pm$ 0.9	73 $\pm$ 1.5	74 $\pm$ 1.2	70 $\pm$ 1.6	60 $\pm$ 1.5

Table 1: The percentage of correct responses in each task before and after training. An improvement in the horizontal task is accompanied by an improvement in the vertical task, and a lack of improvement in the horizontal task is accompanied by a corresponding lack of learning in the vertical task. The numbers in parentheses are the performance of subjects who were called back for additional testing after a significant time break (45 days for observer FL and 10 days for observer YK)

between two notions of novelty:

1. a task is new if an appropriate response function cannot be interpolated from that of familiar examples;
2. a task is new if the units used to compute the response function were not significantly active during familiarization or training.

In some cases (Fiorentini and Berardi, 1981; Fahle and Edelman, 1992), both definitions of novelty apply to the stimuli used to assess transfer of training, and the lack of transfer to these stimuli can be accounted for by models that involve either use-dependent rules or feedback-dependent ones, or both. A further indication that use-dependent synaptic modification may be involved in perceptual learning, has been reported recently by (Karni and Sagi, 1991). In their experiments, subjects performed letter discrimination followed by texture discrimination in the same complex stimulus. Their results show significant learning in the texture task, even though feedback was given only for the letter discrimination.

## 5 Conclusion

The central assumption of the HyperBF approach to the modeling of perceptual function is that the human ability to solve a variety of different perceptual tasks is based on the acquisition of specific input-output examples and on subsequent optimization of the use of the stored examples

with practice. Rationale for this twofold assumption has been provided by the results of simulated psychophysical experiments (Poggio et al., 1992a) that demonstrated that a HyperBF model can learn to solve spatial discrimination tasks with hyperacuity precision, starting from a “tabula rasa” state and continuously improving its performance with repeated exposure to the stimuli.

In the present paper, we concentrated on two computational details of the HyperBF model of vernier acuity. First, we investigated the possibility that oriented spatial filters known to exist in the primate visual system (namely, units similar to the simple cells of Hubel and Wiesel, 1962) can serve as the basis functions in a HyperBF network. Second, we explored the different mechanisms available within the HyperBF framework for incremental learning at the level of the linear combination of basis function activities. Our findings indicate that a simple feedback-independent rule for synaptic modification, that we called EDL, for Exposure-Dependent Learning, may be involved in the improvement of the performance of human subjects with practice.

Both our simulations and our psychophysical data suggest that a significant component of learning in hyperacuity may be based on stimulus-driven feedback-independent amplification of unit responses, rather than on precise feedback-guided fine tuning within a perceptual module. We remark that the perceptual module whose prior availability is assumed by the EDL rule can either be hard-wired from birth, or synthesized in a task-driven fashion, as suggested in (Poggio et al., 1992a). If one accepts the possibility that the visual system is capable of modifying certain aspects of its functional architecture on the fly, the stimulus-driven learning can be given an alternative account in terms of acquisition of new HyperBF centers (T. Poggio, personal communication). It is not clear to us at present whether or not this possibility can be distinguished psychophysically from our account in terms of synaptic modification using existing centers and the EDL rule. The presence of the initial fast stimulus-specific component in the learning curve in hyperacuity tasks (Poggio et al., 1992b) is consistent with the module synthesis view. The record of the last two and a half millennia indicates, however, that the Platonic notion of innate ideas (corresponding, in the present case, to innate perceptual mechanisms tuned by experience) is sufficiently resilient to cope with mere circumstantial evidence to the contrary. It remains to be seen whether a more direct approach, possibly combining physiology with psychophysics and computational modeling, will be more successful in elucidating the nature of perceptual learning.

## Acknowledgments

We thank T. Poggio for stimulating discussions, and two anonymous reviewers for useful and detailed suggestions. YW was supported by the Karen Kupcinet Fund, and by a grant to SE from the Basic Research Foundation, administered by the Israel Academy of Sciences and Humanities.

## References

- Barlow, H. B. (1979). Reconstructing the visual image in space and time. *Nature*, 279:189–190.
- Barto, A. (1989). From chemotaxis to cooperativity: abstract exercises in neuronal learning strategies. In Durbin, R., Miall, C., and Mitchison, G., editors, *The computing neuron*, pages 73–98. Addison Wesley, New York, NY.
- Brown, T. H., Kairiss, E. W., and Keenan, C. L. (1990). Hebbian synapses: biophysical mechanisms and algorithms. *Ann. Rev. Neurosci.*, 13:475–511.
- Crick, F. H. C., Marr, D. C., and Poggio, T. (1981). An information-processing approach to understanding the visual cortex. In Schmitt, F., editor, *The organization of the cerebral cortex*. MIT Press, Cambridge, MA.
- Fahle, M. W. and Edelman, S. (1992). Learning in hyperacuity: influence of stimulus range and of feedback. *Vision Research*. in press.
- Fendick, M. and Westheimer, G. (1983). Effects of practice and the separation of test targets on foveal and perifoveal hyperacuity. *Vision Research*, 23:145–150.
- Fiorentini, A. and Berardi, N. (1981). Perceptual learning specific for orientation and spatial frequency. *Nature*, 287:453–454.
- Hawkins, R. D., Abrams, T. W., Carew, T. J., and Kandel, E. R. (1983). A cellular mechanism of classical conditioning in *aplysia*: Activity-dependent amplification of presynaptic facilitation. *Science*, 219:400–404.
- Hubel, D. H. and Wiesel, T. N. (1962). Receptive fields, binocular interaction and functional architecture in the cat’s visual cortex. *J. Physiol.*, 160:106–154.
- Karni, A. and Sagi, D. (1991). Where practice makes perfect in texture discrimination. *Proceedings of the National Academy of Science*, 88:4966–4970.
- Klein, S. A. and Levi, D. M. (1985). Hyperacuity thresholds of 1 sec: theoretical predictions and empirical validation. *Journal of the Optical Society of America*, A2:1170–1190.
- McKee, S. P. and Westheimer, G. (1978). Improvement in vernier acuity with practice. *Perception and Psychophysics*, 24:258–262.
- Mel, B. W. and Koch, C. (1990). Sigma-Pi learning: on radial basis functions and cortical associative learning. In Touretzky, D., editor, *Neural Information Processing Systems*, volume 2, pages 474–481. Morgan Kaufmann, San Mateo, CA.
- Parker, A. J. and Hawken, M. J. (1985). Capabilities of monkey cortical cells in spatial resolution tasks. *Journal of the Optical Society of America*, 2:1101–1114.

- Parker, A. J. and Hawken, M. J. (1987). Hyperacuity and the visual cortex. *Nature*, 326:105–106.
- Poggio, T., Edelman, S., and Fahle, M. (1992a). Learning of visual modules from examples: a framework for understanding adaptive visual performance. *Computer Vision, Graphics, and Image Processing: Image Understanding*, 56:22–30.
- Poggio, T., Fahle, M., and Edelman, S. (1992b). Fast perceptual learning in visual hyperacuity. *Science*, 256:1018–1021.
- Poggio, T. and Girosi, F. (1990). Regularization algorithms for learning that are equivalent to multilayer networks. *Science*, 247:978–982.
- Shapley, R. and Victor, J. (1986). Hyperacuity in cat retinal ganglion cells. *Science*, 231:999–1002.
- Snippe, H. P. and Koenderink, J. J. (1992). Discrimination thresholds for channel-coded systems. *Biological Cybernetics*, 66:543–551.
- Swindale, N. V. and Cynader, M. S. (1986). Vernier acuity of neurones in cat visual cortex. *Nature*, 319:591–593.
- Walk, R. D. (1978). Perceptual learning. In Carterette, E. C. and Friedman, M. P., editors, *Handbook of Perception*, volume IX, pages 257–298. Academic Press, New York, NY.
- Watt, R. J. and Morgan, M. J. (1985). A theory of primitive spatial code in human vision. *Vision Research*, 25:1661–1674.
- Westheimer, G. (1981). Visual hyperacuity. *Prog. Sensory Physiol.*, 1:1–37.
- Westheimer, G. and McKee, S. P. (1975). Visual acuity in the presence of retinal image motion. *Journal of the Optical Society of America*, 65:847–850.
- Westheimer, G. and McKee, S. P. (1977). Spatial configurations for visual hyperacuity. *Vision Research*, 17:941–947.
- Widrow, B. and Stearns, S. D. (1985). *Adaptive signal processing*. Prentice Hall, Englewood Cliffs, NJ.
- Wilson, H. R. (1986). Responses of spatial mechanisms can explain hyperacuity. *Vision Research*, 26:453–469.
- Wilson, H. R. and Bergen, J. R. (1979). A four mechanism model for threshold spatial vision. *Vision Research*, 19:19–32.
- Wilson, H. R. and Gelb, D. J. (1984). Modified line-element theory for spatial frequency and width discrimination. *Journal of the Optical Society of America*, 1:124–131.